



## Tubulin photoaffinity labeling study with a plinabulin chemical probe possessing a biotin tag at the oxazole

Yuri Yamazaki<sup>a</sup>, Yui Kido<sup>a</sup>, Koushi Hidaka<sup>b</sup>, Hiroyuki Yasui<sup>c</sup>, Yoshiaki Kiso<sup>b</sup>, Fumika Yakushiji<sup>a</sup>, Yoshio Hayashi<sup>a,\*</sup>

<sup>a</sup> Department of Medicinal Chemistry, Tokyo University of Pharmacy and Life Sciences, Hachioji, Tokyo 192-0392, Japan

<sup>b</sup> Department of Medicinal Chemistry, Center for Frontier Research in Medicinal Science, Kyoto Pharmaceutical University, Kyoto 607-8412, Japan

<sup>c</sup> Department of Analytical and Bioinorganic Chemistry, Kyoto Pharmaceutical University, Kyoto 607-8414, Japan

### ARTICLE INFO

#### Article history:

Received 25 September 2010

Revised 23 October 2010

Accepted 26 October 2010

Available online 31 October 2010

#### Keywords:

Anti-cancer agent

Diketopiperazine

Phenylahistin

Tubulin

Vascular disrupting agent

### ABSTRACT

A new bioactive photoaffinity probe KPU-252-B1 (**4**) possessing a biotin tag on the oxazole ring of a potent plinabulin derivative KPU-244 (**2**) was synthesized via the Cu<sup>I</sup>-catalyzed Huisgen's cycloaddition reaction to understand the precise binding mode of the diketopiperazine-based anti-microtubule agent plinabulin on tubulin. Probe **4** showed significant binding affinity toward tubulin and cytotoxicity against an HT-29 cells. A photoaffinity labeling study suggested that probe **4** specifically recognizes tubulin at a binding site that binds plinabulin or colchicine, most likely near or at the colchicine binding site, which is located at the interfacial region formed by  $\alpha$ - and  $\beta$ -tubulin association. The results also demonstrated that probe **4** may serve as a useful plinabulin chemical probe to investigate the molecular mechanism by which anti-microtubule diketopiperazine derivatives operate.

© 2010 Elsevier Ltd. All rights reserved.

## 1. Introduction

Microtubules, which are key components of the cytoskeleton, are noncovalent polymers of  $\alpha$ - and  $\beta$ -tubulin heterodimers (each with a molecular mass of about 50 kDa) that are assembled in a filamentous tube-shaped structure essential to all eukaryotic cells.<sup>1</sup> The cytoskeletal system of eukaryotic cells is an attractive target for anti-cancer chemotherapeutic agents.<sup>2,3</sup> Microtubule targeting agents are generally classified into two main groups. One group, the microtubule-stabilizing agents, stimulates microtubule polymerization and includes paclitaxel, docetaxel, and epothilones. The other group comprises microtubule depolymerizing agents. These compounds inhibit microtubule polymerization and include the *Vinka* alkaloids, colchicine and combretastatins.<sup>2</sup> In particular, colchicine and combretastatin, which recognize the colchicine binding site on tubulin, induce tumor vascular collapse by rapid depolymerization of microtubules in highly proliferating tumor selective vascular endothelial cells.<sup>2</sup> These agents are designated 'vascular disrupting agents' (VDA) and form a promising new class of inducing responses in all solid tumor types in combination therapies.<sup>4</sup>

'Plinabulin' (NPI-2358/KPU-2, **1**, IC<sub>50</sub> of 15 nM against HT-29 cells, Fig. 1), designed and synthesized previously by us from a natural diketopiperazine phenylahistin (PLH, halimide),<sup>5–9</sup> is a potent VDA.<sup>10</sup> Plinabulin is currently being evaluated in Phase II clinical trials in four countries, including the United States. Although PLH exhibits colchicine-like tubulin depolymerizing activity, the chemical structure of plinabulin is different from natural colchicine binding molecules: it has a relatively hydrophilic diketopiperazine (DKP) skeleton. Computer-assisted molecular models of plinabulin and colchicine are not superimposable.<sup>11</sup> Moreover, several biological assays have shown that plinabulin displays properties that are distinct from those of colchicine.<sup>10</sup> Hence, it was attractive to explore the precise binding mode and microtubule depolymerization mechanism of our dehydroDKP-type inhibitor, plinabulin.

In the previous study,<sup>11,12</sup> we demonstrated that plinabulin **1** directly interacted to tubulin with the  $K_d$  value of 1.1  $\mu$ M in the binding assay based on the intrinsic fluorescence quenching of porcine tubulin. To understand the binding mode of plinabulin on tubulin, we performed a photoaffinity labeling study<sup>13</sup> using biotin-tagged photoaffinity probes derived from a benzophenone-containing potent derivative KPU-244 (**2**, IC<sub>50</sub> of 4 nM against HT-29 cells, Fig. 1). We previously synthesized several photoaffinity probes possessing a biotin tag at the 4'-position of the benzophenone moiety of compound **2**.<sup>11,12</sup> Photoaffinity labeling studies of these probes and molecular dynamics (MD) simulations suggested that plinabulin derivatives interact with the boundary

\* Corresponding author. Tel./fax: +81 42 676 3275.

E-mail address: [yhayashi@toyaku.ac.jp](mailto:yhayashi@toyaku.ac.jp) (Y. Hayashi).

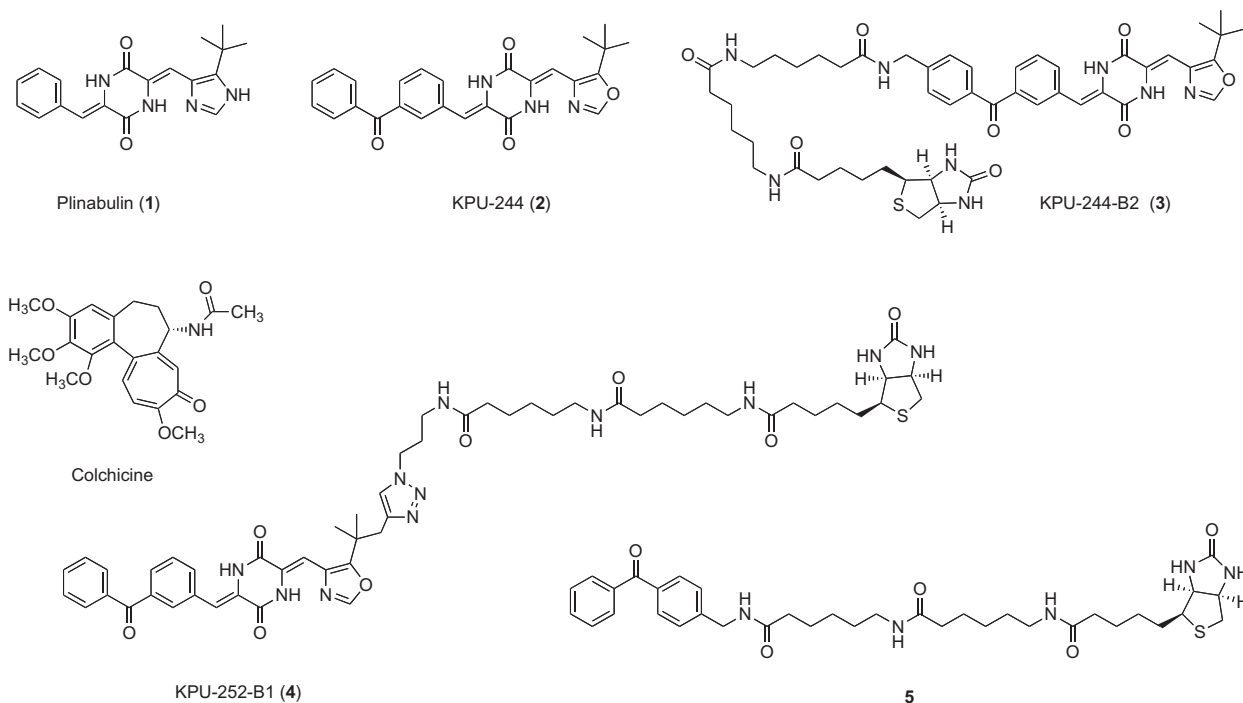


**Figure 1.** Structures of colchicine, plinabulin (1, NPI-2358/KPU-2), KPU-244 (2), KPU-244-B2 (3), a new photoaffinity probe KPU-252-B1 (4), and control compound 5.

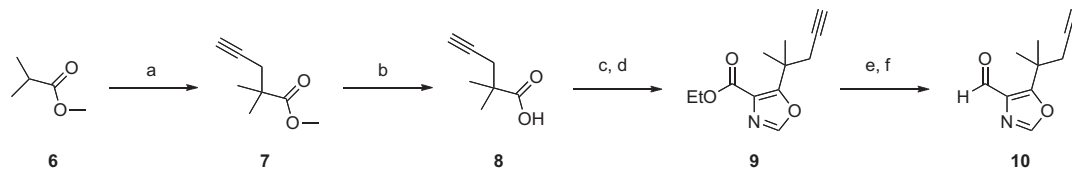
region between the  $\alpha$ - and  $\beta$ -tubulin units at sites that surround the colchicine binding pocket but are not located inside the colchicine binding site. MD simulations indicated the presence of an interfacial pocket formed by  $\alpha$ - and  $\beta$ -tubulin that could accept a biotin tag positioned at the oxazole ring of compound 2, which is located at the opposite side of the benzophenone moiety. Based on these findings, we designed a new plinabulin chemical probe 4 containing a biotin tag at the *tert*-butyl group on the oxazole ring of compound 2. If the MD simulation were accurate, the newly designed probe 4 would function in a manner similar to that of our previous probes. In the synthesis of the new probe 4, we coupled the biotin tag to the plinabulin derivative using the Cu<sup>I</sup>-catalyzed Huisgen's 1,3-dipolar cycloaddition reactions developed by Sharpless and co-workers (click chemistry).<sup>14,15</sup> According to the synthesis shown in Scheme 3, we synthesized the plinabulin derivative 17, which possessed a terminal alkyne, and the biotinyl azide 20. Coupling of these compounds successfully yielded the desired

probe 4. After biological evaluation of the probe 4, tubulin photoaffinity labeling was performed with or without photoirradiation to investigate the binding mode of the probe. The results indicated that probe 4 was a good chemical probe and behaved similarly to our previous probes.

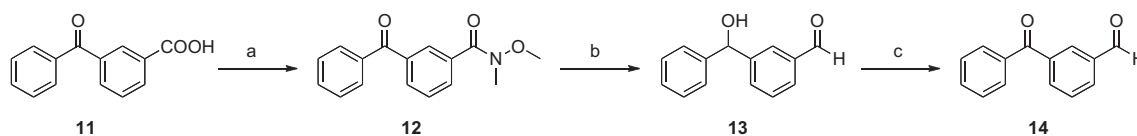
## 2. Results and discussion

### 2.1. Chemistry

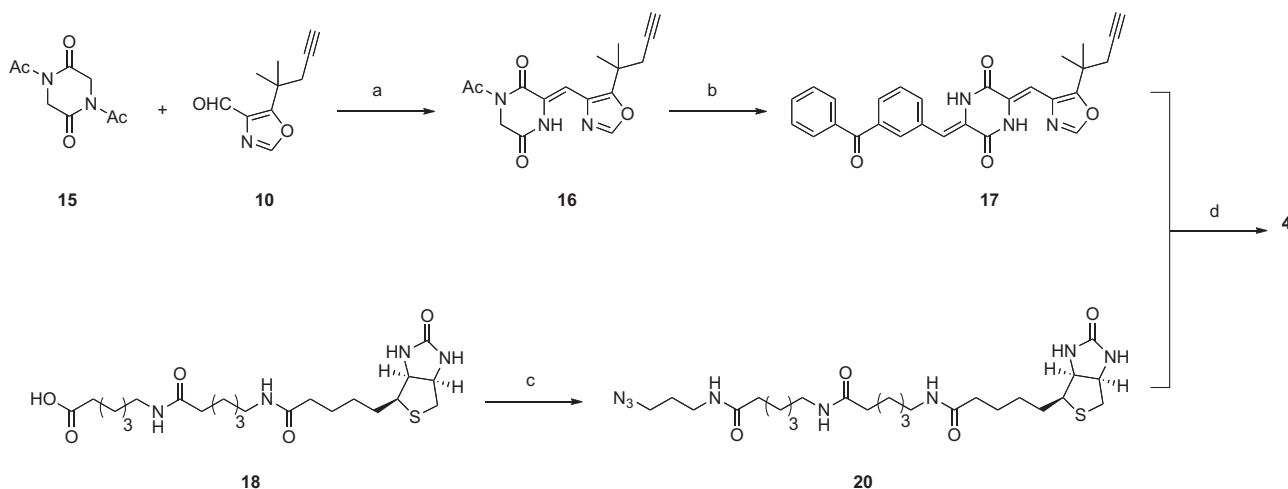
To prepare the photoaffinity probe 4, we first synthesized 5-(2,2-dimethylpent-4-yn-2-yl)oxazole-4-carbaldehyde 10 from methyl isobutyrate 6 in six steps, as described in Scheme 1. After the starting material 6 was treated with lithium diisopropylamide (LDA) at  $-78$  °C, 3-bromopropyne was introduced to an  $\alpha$ -carbon of compound 6 to give the ester 7.<sup>16</sup> The ester 7 was hydrolyzed under



**Scheme 1.** Synthesis of 5-(2-methylpent-4-yn-2-yl)oxazole-4-carbaldehyde 10. Reagents and conditions: (a) 3-bromopropyne, LDA, THF,  $-78$  °C to rt, 59%; (b) 1 M NaOH, CH<sub>3</sub>OH, 65 °C, 92%; (c) DCC, CH<sub>2</sub>Cl<sub>2</sub>, rt; (d) ethyl isocynoacetate, DBU, THF, rt, 69% over two steps; (e) LiAlH<sub>4</sub>, THF,  $-78$  °C; (f) MnO<sub>2</sub>, acetone, rt, 50% over two steps.



**Scheme 2.** Synthesis of 3-benzoylbenzaldehyde 14. Reagents and conditions: (a) MeONHMe-HCl, EDC-HCl, Et<sub>3</sub>N, DMF, rt, 86%; (b) LiAlH<sub>4</sub>, THF,  $-78$  °C, 98%; (c) Dess–Martin periodinane, THF, rt, 87%.



**Scheme 3.** Synthesis of photoaffinity probe **4**. Reagents and conditions: (a)  $\text{Cs}_2\text{CO}_3$ , DMF, rt, 57%; (b) **14**,  $\text{Cs}_2\text{CO}_3$ , DMF, 60 °C, 61%; (c) 3-azido-propylamine **19**, EDC-HCl, HOBT-H<sub>2</sub>O, DMF/DMSO, rt, then HPLC purification, 25%; (d) 5 mol %  $\text{Cu}(\text{OAc})_2$ , 15 mol % sodium ascorbate, H<sub>2</sub>O/*t*-butanol/DMF, MW, 80 °C, 15 min, then HPLC purification, 63%.

basic conditions to afford the corresponding carboxylic acid **8**. After the carboxylic acid **8** was converted to the corresponding anhydride with *N,N'*-dicyclohexylcarbodiimide (DCC), the resultant anhydride and ethyl isocynoacetate were condensed in the presence of 1,8-diazabicyclo[5.4.0]undec-7-ene (DBU) to afford oxazolecarboxylate **9**.<sup>17</sup> This ester **9** was subsequently reduced with  $\text{LiAlH}_4$  to yield the corresponding oxazole carbinol, followed by oxidation with  $\text{MnO}_2$  to give the desired aldehyde **10**.

**Scheme 2** shows that compound **17** was synthesized from 3-benzoylbenzaldehyde **14** as follows: the purchased benzoylbenzoic acid **11** was converted to the corresponding Weinreb amide **12**, followed by reduction with  $\text{LiAlH}_4$  to obtain benzhydryl alcohol **13**. This alcohol **13** was then oxidized with Dess–Martin periodinane<sup>18</sup> to yield the desired aldehyde **14**.

To obtain the biotin-tagged derivative **4** as a photoaffinity probe, we separately synthesized two units, namely, DKP part **17** and biotinyl azide **20**, which were then conjugated by Huisgen's cycloaddition, as described in **Scheme 3**. During synthesis of the DKP part **17** core structure of the anti-microtubule activity, oxazolecarboxaldehyde **10** was condensed to *N,N*-diacetyl piperazine-2,5-dione **15** in the presence of  $\text{Cs}_2\text{CO}_3$  in *N,N*-dimethylformamide (DMF) under an argon atmosphere<sup>19</sup> to give mono-dehydroDKP **16**. The second aldehyde **14** was introduced, by a similar aldol reaction, to mono-dehydroDKP **16** to afford alkylnyl di-dehydroDKP **17**. In the synthesis of the linker part, biotin-Acp-Acp-OH **18** (Acp: aminocaproyl) was prepared by Fmoc-based solid phase chemistry using the procedure described previously.<sup>12</sup> 3-Azido propylamine **19** was prepared from 3-bromo-1-propylamine hydrobromide by azidation.<sup>20</sup> Azidation to yield compound **19** was confirmed by observation of a strong absorption at  $2098\text{ cm}^{-1}$  in the FT-IR spectrum. Coupling between the biotinyl peptide **18** and azido propylamine **19** was performed using the EDC-HOBt method, and the crude products were purified by preparative HPLC to afford the desired biotinyl azide **20**.

Finally, Huisgen's cycloaddition was performed between the alkylnyl di-dehydroDKP **17** and the biotinyl azide **20** in the presence of 5 mol %  $\text{Cu}(\text{OAc})_2$  and 15 mol % sodium ascorbate in water/*t*-butanol/DMF under microwave irradiation to shorten the reaction time and increase the chemical yield.<sup>21</sup> After microwave irradiation, a new single peak was detected in the reverse phase HPLC analysis. Thus, the reaction mixture was purified by preparative HPLC to afford the desired probe **4** in 63% yield. The observed relatively low yield in the  $\text{Cu}^I$ -catalyzed cycloaddition was due to the low solubility of the biotinyl azide **20**.

Compound **5** (**Fig. 1**), a negative control compound for the photoaffinity labeling study, was also prepared. Synthesis of this compound has been described previously.<sup>11</sup>

## 2.2. Biological activity of probe 4

The biological activity of the synthetic photoaffinity probe **4** was evaluated first by performing a binding assay against purified porcine tubulin (0.5  $\mu\text{M}$ ) in MES buffer (pH 6.8) at 37 °C.<sup>22</sup> The dissociation constant ( $K_d$ ) of the probe **4** was calculated to be 17.9  $\mu\text{M}$  (**Fig. 2**). The binding affinity of probe **4** was about 17 times and 5 times less than the binding affinities of plinabulin **1** (1.06  $\mu\text{M}$ )<sup>12</sup> and colchicine (3.70  $\mu\text{M}$ , **Fig. S1 in the Supplementary data**), respectively. Compound **5**, the negative control, did not bind to tubulin at all (**Fig. S2 in the Supplementary data**). The binding affinity of probe **4** was found to be significant. Next, an *in vitro* cytotoxicity assay was performed based on the XTT/PMS method.<sup>23</sup> In this method, probe **4** showed low but significant cytotoxicity against the HT-29 human colon cancer cell lines with an  $\text{IC}_{50}$  value of 9.8  $\mu\text{M}$  (**Table 1**), 725 times less potent than plinabulin **1** (13.5 nM, **Table 1**). The higher molecular weight and greater hydrophilicity of probe **4** probably resulted in poor cellular uptake, which reduced the cytotoxicity. These findings together indicated that probe **4** may be valuable in a subsequent photoaffinity labeling study.

## 2.3. Tubulin photoaffinity labeling

The binding site of probe **4** was investigated by photoaffinity labeling to tubulin. Purified porcine tubulin was photo-irradiated at 365 nm in the presence or absence of probe **4** on ice after incubation at 37 °C in MES buffer (containing 1 mM GTP, pH 6.8) for the appropriate duration. The sample was then separated by SDS-PAGE using a 10% polyacrylamide gel. The protein was transferred to a PVDF membrane, and the photolabeled protein, to which was attached probe **4**, was visualized using a streptavidin-HRP/ECL system. Non-specific binding was very low in the absence of photo-irradiation (lanes 1 and 9 in **Fig. 3**), suggesting that chemical modification of tubulin through covalent bond formation (e.g., Michael addition reaction) with probe **4** did not occur. In the photo-irradiated samples, UV irradiation time- or dose-dependent labeling was observed (lanes 2–4 and 10–12 in **Fig. 3**, respectively). Non-specific photolabeling by the benzophenone moiety on probe **4** was assessed by photoaffinity labeling with compound **5**, which did not show any binding activity to tubulin in the binding assay

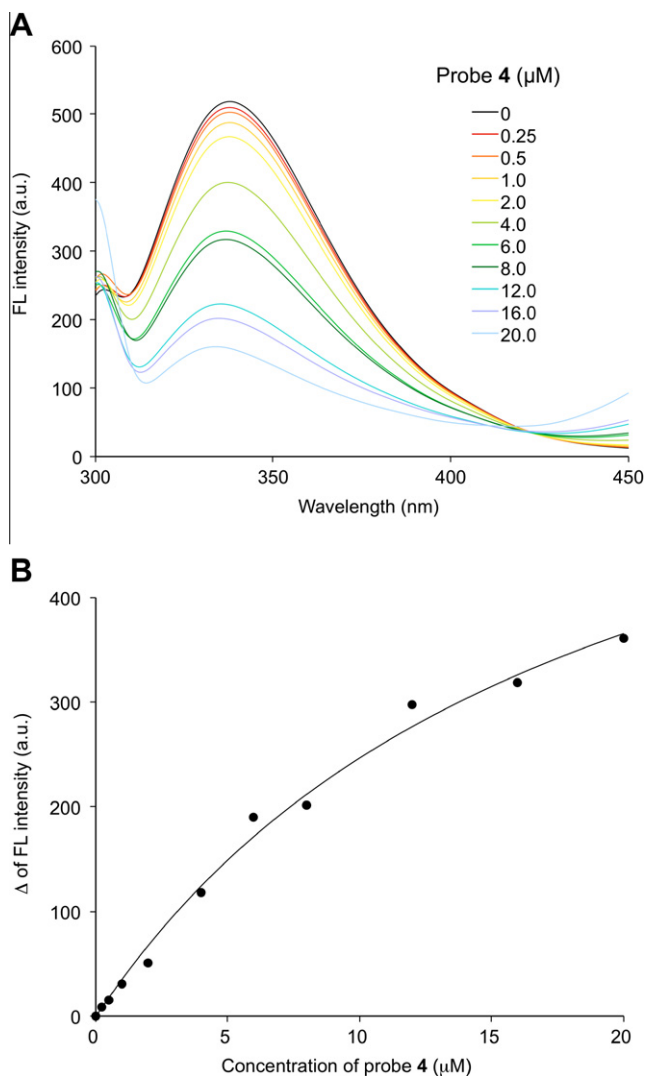


**Figure 2.** Tubulin binding assay based on fluorescence quenching. (A) Fluorescence quenching on tubulin by probe **4**. (B) Increase of tubulin-probe **4** binding complex.

**Table 1**  
Tubulin binding activity and cytotoxicity of compounds

Compounds	$K_d^a$ ( $\mu\text{M}$ )	$\text{IC}_{50}^b$ (nM)
Plinabulin <b>1</b>	$1.06 \pm 0.18$	$13.5 \pm 2.2$
Probe <b>4</b>	$17.9 \pm 3.4$	$9788 \pm 1680$
Colchicine	$3.70 \pm 0.18$	$16.6 \pm 0.9$

<sup>a</sup> Porcine tubulin concentration: 0.5  $\mu\text{M}$ .

<sup>b</sup>  $\text{IC}_{50}$  against HT-29 cells. Experiments were triplicated.

described above. In this case, only weakly stained bands were detected, in contrast with the case of probe **4** labeling, and the staining was not UV irradiation-time-dependent. It would appear that the observed weak bands could be attributed to non-specific photolabeling.

A competitive photoaffinity labeling study using probe **4** was carried out in the presence or absence of plinabulin **1**, colchicine, vinblastine, or D-biotin to elucidate the binding mode of probe **4** on tubulin (Fig. 3 and densitometry analysis is shown in Fig. S6, Supplementary data). Dose-dependent inhibition of photoaffinity labeling was observed in the presence of plinabulin **1** (1–50 equiv, lanes 21–24 in Fig. 3D), indicating that probe **4** recognized the same binding site as plinabulin **1**. Photoaffinity labeling with probe **4** was also inhibited dose-dependently (5–100 equiv) in the presence of colchicine (lanes 13–16 in Fig. 3C) but not in the presence of D-biotin

as a negative control (5–100 equiv, lanes 17–20 in Fig. 3C). This result was consistent with a previous report that PLH, an original lead compound of plinabulin **1**, competed with [ $^3\text{H}$ ]colchicine for tubulin.<sup>6</sup> When vinblastine, an anti-microtubule agent that recognizes a binding site (the vinblastine site) that is distinct from the colchicine binding site, was used in high concentration as a competitor, moderate inhibition was observed (lanes 26–28 in Fig. 3D). This could be attributed to an allosteric effect of vinblastine binding to its own binding site, which induces small conformational changes at the colchicine binding site,<sup>24</sup> or a vinblastine-induced paracrystal formation of tubulin,<sup>25</sup> leading to the inhibition of probe **4** binding. Therefore, it has been comprehensively demonstrated that plinabulin and colchicine recognized the probe **4** binding site, suggesting that the new probe **4** may be used effectively for investigating the properties of the plinabulin binding site. In our previous study, we developed other plinabulin chemical probes KPU-244-B2 (**3**) and -B3, which featured a biotin tag at the benzophenone moiety, in contrast with probe **4**, which features a biotin tag at the opposite oxazole side.<sup>11,12</sup> In both cases, it was concluded that these chemical probes recognized tubulin in a similar manner.

In consideration for the fact that the probes possessing biotin tags at different positions on a common structure may recognize tubulin in a similar manner, it was speculated that the interfacial structure formed by the  $\alpha$ - and  $\beta$ -tubulin subunits included a space for accepting not only the DKP core structure, but also the biotin linkers located on different parts of the tubulin. The binding modes of KPU-244-B2 (**3**) and -B3 were previously analyzed in a docking study.<sup>12</sup> Hence, in the present study, the binding mode of probe **4** at the colchicine binding site was assessed by performing a similar docking study using the molecular modeling package MOE 2009.10 (Chemical Computing Group, Inc., Montreal, Canada). Tubulin proteins were modeled according to the crystallographic data of the complex with colchicine (PDB ID, 1SA0). Because probe **4** successfully formed a photolabel and exhibited functions similar to probe **3**, probe **4** was assumed to dock proximal to the colchicine binding site of the tubulin dimer, and initial conformation of **4** was built using previous result of **2**.<sup>12</sup> Next, an energy minimization routine and MD simulation were successively performed. In the obtained model, probe **4** was found to be positioned at the boundary region between the  $\alpha$ - and  $\beta$ -tubulin subunits, a region that partially overlapped with the colchicine binding pocket (Fig. 4). The 2,2-dimethyl group on probe **4** covered the colchicine binding pocket, indicated in green on the molecular surface shown in Fig. 4, and the benzophenone moiety was situated slightly closer to the  $\beta$ -tubulin than in the case of probe **3** docking. In addition, the model suggested that the biotin linker on probe **4** protruded from the interfacial region away from the tubulin molecule through the interfacial space formed between the  $\alpha$ - and  $\beta$ -subunits, although the orientation of the biotin linker on probe **4** differed from that of probe **3**. Therefore, probe **4** appears to specifically recognize tubulin and functions as an effective chemical probe in a manner similar to that of probe **3**. Our anti-microtubule diketopiperazine derivatives may bind at the boundary region formed between the  $\alpha$ - and  $\beta$ -tubulin subunits around the colchicine binding site, but not inside the site, to effectively disrupt the interaction between the two tubulin subunits, thereby producing microtubule depolymerization. Further analysis using the photoaffinity probes is now under way to identify the modified amino acid residues that react with the photoaffinity probe. These findings would help us understand the mechanism of binding between plinabulin derivatives and tubulin.

### 3. Conclusion

We designed and synthesized a new bioactive photoaffinity probe KPU-252-B1 (**4**) possessing a biotin tag on the oxazole ring

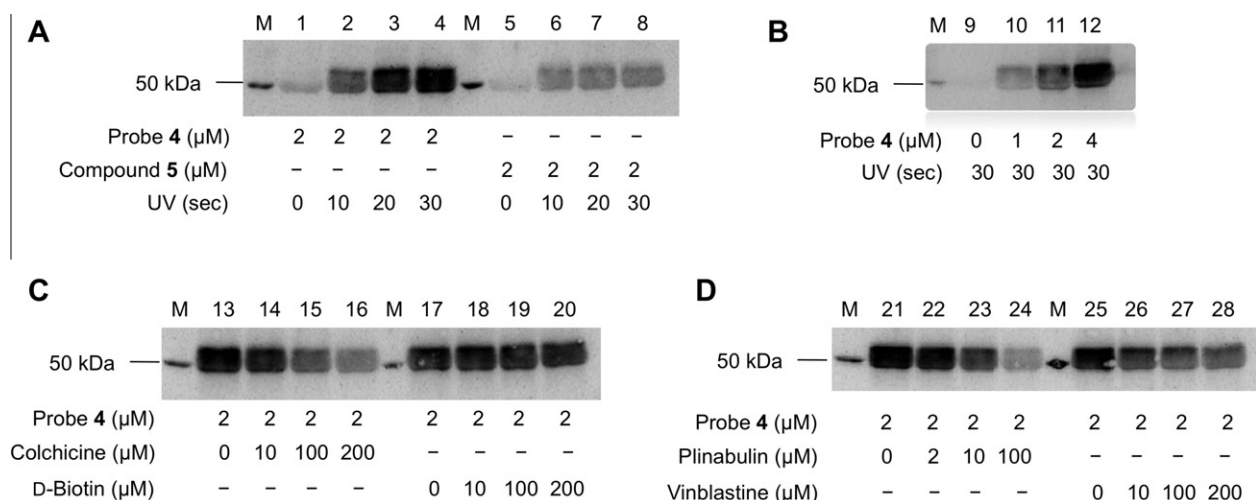


**Figure 3.** Photoaffinity labeling of tubulin. (A) Photoaffinity labeling with probe 4 (2 μM) or compound 5 (2 μM) at different irradiation times. Porcine tubulin was incubated with probe 4 or compound 5 at 37 °C in MES buffer, followed by photo-irradiation for the appropriate time (0–30 s). (B) Photoaffinity labeling in the presence of different concentrations of probe 4 (1–4 μM). (C) Photoaffinity labeling with probe 4 (2 μM) in the absence (lanes 13 and 17) or presence (10–200 μM, lanes 14–16) of colchicine or D-biotin (10–200 μM, lanes 18–20). Samples were photo-irradiated for 30 s. (D) Photoaffinity labeling with probe 4 (2 μM) in the absence (lanes 21 and 25) or presence of plinabulin 1 (2–100 μM, lanes 22–24) or vinblastine (10–200 μM, lanes 26–28). Samples were photo-irradiated for 30 s.

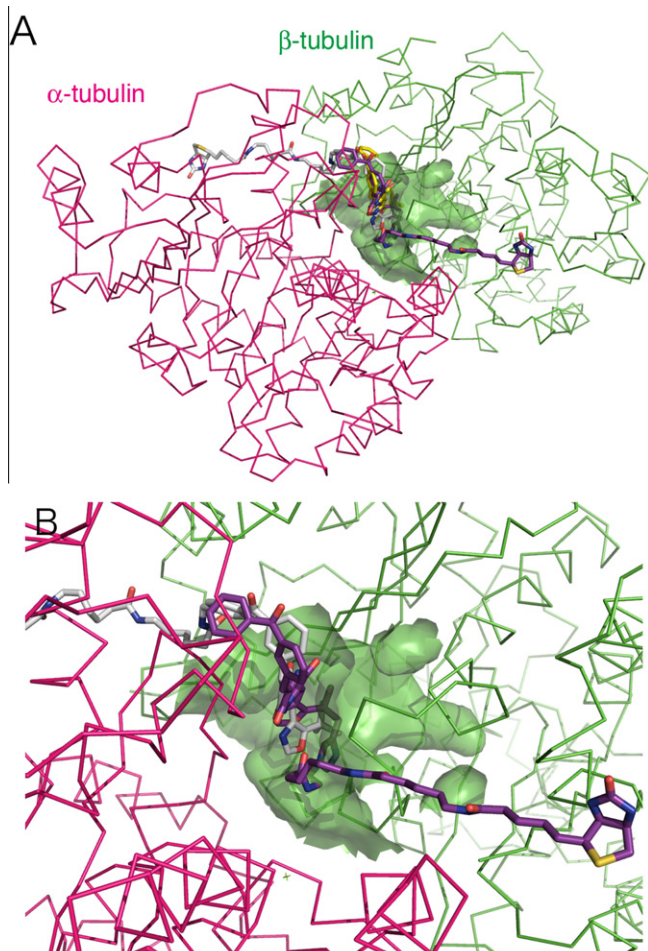


**Figure 4.** Superimposition of molecular dynamics simulated probe 4 (purple sticks) and probe 3 (KPU-244-B2, white sticks) in a tubulin heterodimer constructed from KPU-244 (2, yellow sticks). (A) Full view of probe 4. α- and β-Tubulin are represented by the magenta and green ribbons, respectively. The colchicine binding site on β-tubulin is represented by the green surface. (B) Close-up view of the binding area.

of a potent plinabulin derivative KPU-244 (2) via the Cu<sup>I</sup>-catalyzed Huisgen's cycloaddition reaction. Probe 4 exhibited significant binding affinity toward tubulin and cytotoxicity against an HT-29 cells. Furthermore, probe 4 photolabeled tubulin in a dose- or UV irradiation-time-dependent manner, and labeling was inhibited by addition of colchicine or plinabulin. These results revealed that probe 4 serves as an effective chemical probe of our anti-microtubule diketopiperazines, and its recognition site is located around the intradimer space between the α- and β-tubulin units, near the colchicine binding site. These results are consistent with our previous findings based on a photoaffinity labeling study using other plinabulin chemical probes. Therefore, our synthetic probes may contribute to an understanding of the tubulin depolymerization activity of diketopiperazine-based anti-microtubule agent, plinabulin.

## 4. Experimental

### 4.1. General

Reagents and solvents were purchased from Wako Pure Chemical Ind., Ltd (Osaka, Japan), Nakalai Tesque (Kyoto, Japan), and Aldrich Chemical Co. Inc. (Milwaukee, WI, USA) and were used without further purification. Porcine tubulin was purchased from Cytoskeleton, Inc. (Denver, Colorado, USA). All other chemicals were of the highest commercially available purity. Analytical thin-layer chromatography (TLC) was performed on Merck silica gel 60F<sub>254</sub> pre-coated plates. Preparative HPLC was performed using a C18 reverse-phase column (19 × 100 mm; SunFire™ Prep C18 OBD™ 5 μm) with a binary solvent system: a linear gradient of CH<sub>3</sub>CN in 0.1% aqueous TFA at a flow rate of 10 mL/min, detected at UV 230 nm and 365 nm. Solvents used for HPLC were HPLC-grade. <sup>1</sup>H and <sup>13</sup>C NMR spectra were recorded on either a JEOL JNM-AL300 or a Varian Mercury 300 spectrometers at 300 and 75 MHz, or a BRUKER AV600 spectrometer at 600 MHz. Chemical shifts were recorded as δ values in parts per million (ppm) downfield from tetramethylsilane (TMS). High-resolution mass spectra (EI, CI) were recorded on a JEOL JMS-GCmate, and high-resolution mass spectra (ESI) were recorded on a micromass Q-ToF Ultima API. Photoaffinity labeling was performed using UV Spot Light Source L9588-01 (Hamamatsu Photonics).

## 4.2. Synthesis of compounds 4, 7–10, 12–14, 16, 17, 19, and 20

### 4.2.1. Methyl 2,2-dimethyl pent-4-ynoate (7) [CAS No. 86101-49-7]<sup>16</sup>

To a solution of methyl isobutyrate (8 g, 78 mmol) in anhydrous THF (50 mL) was added dropwise a 1.8 M solution of LDA solution in THF (47 mL, 85.8 mmol) at  $-78^{\circ}\text{C}$  under an argon atmosphere, and the mixture was stirred for 1 h at the same temperature. To this solution was then slowly added a solution of 3-bromopropyne (9.7 g, 82 mmol) in anhydrous THF (8 mL) at  $-78^{\circ}\text{C}$  under an argon atmosphere. The cooling bath was removed, the mixture was stirred overnight at room temperature, and the reaction mixture was quenched with water (50 mL). The organic layer was separated, and the aqueous layer was extracted once with  $\text{Et}_2\text{O}$ . The combined organic layers were washed with brine, dried over  $\text{Na}_2\text{SO}_4$ , and concentrated in vacuo. Distillation of the residual oil at  $55\text{--}60^{\circ}\text{C}$  (20 mmHg) gave a colorless oil (6.5 g, 59%) of compound **7**.  $^1\text{H}$  NMR (300 MHz,  $\text{CDCl}_3$ )  $\delta$  1.28 (s, 6H), 2.01 (t, 1H,  $J = 2.6$  Hz), 2.45 (d, 2H,  $J = 2.6$  Hz), 3.70 (s, 3H).

### 4.2.2. 2,2-Dimethyl pent-4-ynoic acid (8)

A suspension of compound **7** (1.0 g, 7.13 mmol) in methanol (10 mL) and 1 M NaOH (11 mL) was stirred for 4 h at  $60^{\circ}\text{C}$ . After cooling to room temperature, the reaction mixture was acidified by addition of excess 6 M HCl and extracted five times with  $\text{Et}_2\text{O}$ . The combined organic layers were washed with brine, dried over  $\text{Na}_2\text{SO}_4$ , and concentrated in vacuo to give a colorless oil of compound **8** (0.83 g, 92%).  $^1\text{H}$  NMR (300 MHz,  $\text{CDCl}_3$ )  $\delta$  1.32 (s, 6H), 2.04 (t, 1H,  $J = 2.6$  Hz), 2.47 (d, 2H,  $J = 2.6$  Hz).

### 4.2.3. Ethyl 5-(2-methylpent-4-yn-2-yl)oxazole-4-carboxylate (9)

To a solution of compound **8** (0.8 g, 6.34 mmol) in anhydrous dichloromethane (4 mL) was added DCC (654 mg, 3.17 mol), and the mixture was stirred for 4 h at room temperature. After dicyclohexylurea was filtered off in a glass filter and rinsed with a small amount of dichloromethane, the organic solvent was concentrated in vacuo and the resulting DCU was removed on a glass filter. The filtrate was concentrated in vacuo to give a yellow oil of the corresponding anhydride (0.61 g, 82%). This oil was used in the next reaction without further purification. According to the report by Suzuki et al.,<sup>17</sup> to the solution of ethyl isocynoacetate (271 mg, 2.4 mmol) in anhydrous THF (9 mL) were added DBU (365 mg, 2.4 mmol) and the anhydride (0.56 g, 2.4 mmol), and the mixture was stirred at room temperature overnight. After the solvent was removed in vacuo, the residue was extracted with EtOAc, washed with 10%  $\text{Na}_2\text{CO}_3$ , 10% citric acid, and brine, dried over  $\text{Na}_2\text{SO}_4$ , and concentrated in vacuo. The residual oil was purified by silica gel column chromatography using hexane/EtOAc (6:1–5:1) as the eluent to give a colorless oil of compound **9** (367 mg, 69%).  $^1\text{H}$  NMR (300 MHz,  $\text{CDCl}_3$ )  $\delta$  1.42 (t, 3H,  $J = 7.1$  Hz), 1.54 (s, 6H), 1.90 (t, 1H,  $J = 2.6$  Hz), 2.83 (d, 2H,  $J = 2.6$  Hz), 4.39 (q, 2H,  $J = 7.1$  Hz), 7.75 (s, 1H); HRMS (ESI):  $m/z$  222.1124 ( $\text{M}+\text{H}^+$ ) (calcd for  $\text{C}_{12}\text{H}_{16}\text{NO}_3$ : 222.1130).

### 4.2.4. 5-(2-Methylpent-4-yn-2-yl)oxazole-4-carbaldehyde (10)

To a solution of ester **9** (1.31 g, 6.0 mol) in anhydrous THF (50 mL) was added portionwise  $\text{LiAlH}_4$  (225 mg, 6.0 mmol) at  $-78^{\circ}\text{C}$  under an argon atmosphere, and the bath temperature was gradually increased to  $-35^{\circ}\text{C}$  with stirring for 2.5 h. After the mixture was quenched with satd  $\text{NH}_4\text{Cl}$  at  $-78^{\circ}\text{C}$ , EtOAc was added and the resulting precipitate was removed by Celite filtration. The filtrate was washed with  $\text{H}_2\text{O}$  and brine, dried over  $\text{Na}_2\text{SO}_4$ , and concentrated in vacuo to give an oil of the corresponding oxazole alcohol (1.22 g). This oil was used in the next oxidation without further purification. To a solution of the oxazole alcohol (1.22 g, 6.8 mmol) in acetone (54 mL) was added  $\text{MnO}_2$  (3.0 g,

34 mmol), and the mixture was stirred at room temperature overnight. After the  $\text{MnO}_2$  was removed by filtering, the solvent was removed in vacuo and the residual oil was purified by silica gel column chromatography using hexane/EtOAc (4:1–3:1) as an eluent to give a yellow oil of compound **10** (530 mg, 50%).  $^1\text{H}$  NMR (300 MHz,  $\text{CDCl}_3$ )  $\delta$  1.54 (s, 6H), 1.94 (t, 1H,  $J = 2.6$  Hz), 2.72 (d, 2H,  $J = 2.6$  Hz), 7.80 (s, 1H), 10.07 (s, 1H); HRMS (ESI):  $m/z$  178.0856 ( $\text{M}+\text{H}^+$ ) (calcd for  $\text{C}_{10}\text{H}_{12}\text{NO}_2$ : 178.0868).

### 4.2.5. 3-Benzoyl-N-methoxy-N-methylbenzamide (12)

To the solution of 3-benzoylbenzoic acid **11** (850 mg, 3.76 mmol) in DMF (40 mL) were added *N,O*-dimethyl hydroxylamine hydrochloride (385 mg, 3.95 mmol),  $\text{Et}_3\text{N}$  (0.55 mL, 3.95 mmol), and EDC-HCl (757 mg, 3.95 mmol). After the mixture was stirred for 5 h at room temperature, the solvent was removed in vacuo and the residue was dissolved in EtOAc, washed with 10% citric acid, 10%  $\text{NaHCO}_3$ , and brine, dried over  $\text{Na}_2\text{SO}_4$ . The solvent was removed in vacuo to give a colorless oil of compound **12** (0.95 g, 86%).  $^1\text{H}$  NMR (300 MHz,  $\text{CDCl}_3$ )  $\delta$  3.37 (s, 3H), 3.56 (s, 3H), 7.46–7.60 (m, 4H), 7.78–7.81 (m, 2H), 7.91 (dd, 2H,  $J = 1.6$ , 7.5 Hz), 8.09 (t, 1H,  $J = 1.5$  Hz);  $^{13}\text{C}$  NMR (75.5 MHz,  $\text{CDCl}_3$ )  $\delta$  33.5, 61.2, 128.2, 128.4, 129.7, 130.0, 131.9, 132.0, 132.7, 134.2, 137.1, 137.4, 168.9, 196.0; HRMS (EI):  $m/z$  269.1045 ( $\text{M}^+$ ) (calcd for  $\text{C}_{16}\text{H}_{15}\text{NO}_3$ : 269.1052).

### 4.2.6. 3-(Hydroxy(phenyl)methyl)benzaldehyde (13)

To a solution of Weinreb amide **12** (505 mg, 1.87 mmol) in anhydrous THF (15 mL) was added portionwise  $\text{LiAlH}_4$  (85.4 mg, 2.25 mmol) at  $-78^{\circ}\text{C}$  under an argon atmosphere, and the mixture was stirred for 2.5 h at the same temperature. After the mixture was quenched with  $\text{H}_2\text{O}$  at  $-78^{\circ}\text{C}$ , EtOAc was added and the resulting precipitate was removed by Celite filtration. The filtrate was washed with  $\text{H}_2\text{O}$  and brine, dried over  $\text{Na}_2\text{SO}_4$ , and concentrated in vacuo to give an oil of compound **13** (390 mg, 98%).  $^1\text{H}$  NMR (300 MHz,  $\text{CDCl}_3$ )  $\delta$  2.39 (d, 1H), 5.92 (d, 1H), 7.27–7.37 (m, 5H), 7.49 (t, 1H,  $J = 7.7$  Hz), 7.66 (d, 1H,  $J = 7.7$  Hz), 7.78 (d, 1H,  $J = 7.7$  Hz), 7.92 (s, 1H), 9.98 (s, 1H);  $^{13}\text{C}$  NMR (75.5 MHz,  $\text{CDCl}_3$ )  $\delta$  75.7, 126.6, 127.6, 128.0, 128.8, 129.2, 132.5, 136.5, 143.2, 144.9, 192.3; HRMS (CI):  $m/z$  213.0924 ( $\text{M}+\text{H}^+$ ) (calcd for  $\text{C}_{14}\text{H}_{13}\text{O}_2$ : 213.0915).

### 4.2.7. 3-Benzoylbenzaldehyde (14)

To a solution of aldehyde **13** (102 mg, 0.48 mmol) in THF (5 mL) was added Dess–Martin periodinane (305 mg, 0.72 mmol), and the mixture was stirred for 2 h at room temperature. After the mixture was quenched by the addition of satd  $\text{NaHCO}_3$  (1.5 mL) and satd  $\text{Na}_2\text{S}_2\text{O}_3$  (1.5 mL), EtOAc was added, and the organic layer was washed with brine, dried over  $\text{Na}_2\text{SO}_4$ , and concentrated in vacuo. The residual oil was purified by silica gel column chromatography using hexane/EtOAc (4:1) as an eluent to give a colorless oil of compound **14** (88 mg, 87%).  $^1\text{H}$  NMR (300 MHz,  $\text{CDCl}_3$ )  $\delta$  7.51 (dd, 2H,  $J = 7.7$ , 7.1 Hz), 7.61–7.71 (m, 2H), 7.79–7.83 (m, 2H), 8.07–8.13 (m, 2H), 8.28 (t, 1H,  $J = 1.6$  Hz), 10.09 (s, 1H);  $^{13}\text{C}$  NMR (75.5 MHz,  $\text{CDCl}_3$ )  $\delta$  128.6, 129.2, 130.0, 131.3, 132.6, 133.0, 135.4, 136.3, 136.8, 138.5, 191.4, 195.4; HRMS (EI):  $m/z$  210.0684 ( $\text{M}^+$ ) (calcd for  $\text{C}_{14}\text{H}_{10}\text{O}_2$ : 210.0681).

### 4.2.8. (Z)-1-Acetyl-3-((5-(2-methylpent-4-yn-2-yl)oxazol-4-yl)methylene)piperazine-2,5-dione (16)

To a solution of aldehyde **10** (46.5 mg, 0.262 mmol) in anhydrous DMF (5 mL) was added *N,N'*-diacetyl-2,5-diketopiperazine-2,5-dione (**15**, 78 mg, 0.394 mmol). The solution was repeatedly evacuated for short periods of time to remove oxygen, then flushed with argon. To this solution was added  $\text{Cs}_2\text{CO}_3$ , and the evacuation–flushing process was repeated again. An argon atmosphere was maintained throughout the reaction. The resultant mixture

was stirred at room temperature overnight. After the solvent was removed in vacuo, the residue was extracted with EtOAc, washed with H<sub>2</sub>O and brine, dried over Na<sub>2</sub>SO<sub>4</sub>, and concentrated in vacuo. The residual oil was purified by silica gel column chromatography using CHCl<sub>3</sub>/MeOH (100:1) as an eluent to give a pale yellow powder of compound **16** (47 mg, 57%). <sup>1</sup>H NMR (300 MHz, CDCl<sub>3</sub>) δ 1.55 (s, 6H), 2.00 (t, 1H, *J* = 2.6 Hz), 2.59 (d, 2H, *J* = 2.6 Hz), 2.65 (s, 3H), 4.48 (s, 2H), 7.08 (s, 1H), 7.87 (s, 1H), 11.23 (br s, 1H); HRMS (ESI): *m/z* 316.1300 (M+H<sup>+</sup>) (calcd for C<sub>16</sub>H<sub>18</sub>N<sub>3</sub>O<sub>4</sub>: 316.1297).

#### 4.2.9. (3Z,6Z)-3-(3-Benzoylbenzylidene)-6-((5-(2-methyl-pent-4-yn-2-yl)oxazol-4-yl)methylene)piperazine-2,5-dione (**17**)

To a solution of monodehydroDKP **16** (4 mg, 0.0127 mmol) in anhydrous DMF (2 mL) were added Cs<sub>2</sub>CO<sub>3</sub> (8.3 mg, 0.0254 mmol) and aldehyde **14** (5.34 mg, 0.0254 mmol) under an argon atmosphere, and the mixture was stirred for 3 h at 60 °C. After the solvent was removed in vacuo, the residue was extracted with EtOAc, washed with 10% citric acid, 5% NaHCO<sub>3</sub>, and brine, dried over Na<sub>2</sub>SO<sub>4</sub>, and concentrated in vacuo. The residual oil was purified by preparative HPLC (with a linear gradient of 50–90% CH<sub>3</sub>CN in 0.1% aq TFA over 40 min) to give a pale yellow powder of didehydroDKP **17** (3.6 mg, 61%). <sup>1</sup>H NMR (300 MHz, DMSO-*d*<sub>6</sub>) δ 1.47 (s, 6H), 2.60 (d, 2H, *J* = 2.3 Hz), 2.89 (t, 1H, *J* = 2.3 Hz), 6.72 (s, 1H), 6.87 (s, 1H), 7.56–7.84 (m, 9H), 8.66 (s, 1H), 10.62 (s, 1H), 11.14 (s, 1H); HRMS (ESI): *m/z* 466.1760 (M+H<sup>+</sup>) (calcd for C<sub>28</sub>H<sub>24</sub>N<sub>3</sub>O<sub>4</sub>: 466.1767).

#### 4.2.10. 3-Azido-propylamine (**19**) [CAS No. 109-76-2]<sup>20</sup>

To a solution of 3-bromo-1-propylamine hydrobromide (1.6 g, 7.3 mmol) in water (5 mL) was slowly added a solution of sodium azide (1.6 g, 24.6 mmol) in water (7.5 mL), and the mixture was refluxed overnight. After cooling to room temperature, about one-half of the water was removed by evaporation in vacuo, and the remaining residue was diluted with Et<sub>2</sub>O. This biphasic mixture was cooled to 0 °C and KOH pellets (2.0 g) were slowly added. The phases were separated and the aqueous layer was extracted twice with Et<sub>2</sub>O. The combined organic layers were dried over MgSO<sub>4</sub> and concentrated in vacuo to give a yellow oil of **19** (412 mg, 56%). <sup>1</sup>H NMR (300 MHz, CDCl<sub>3</sub>) δ 1.29 (br s, 2H), 1.69–1.78 (m, 2H), 2.81 (t, 2H, *J* = 6.9 Hz), 3.38 (t, 2H, *J* = 6.7 Hz).

#### 4.2.11. N-D-Biotinyl-Acp-Acp-amino-propylazide (**20**)

To a solution of D-biotin-Acp-Acp-OH (54 mg, 0.114 mmol) in DMF/DMSO (5 mL) were added HOBt·H<sub>2</sub>O (16 mg, 0.114 mmol), EDC·HCl (22 mg, 0.114 mmol), and 3-azido propylamine (23 mg, 0.228 mol), and the mixture was stirred at room temperature overnight. The resultant precipitates were collected and washed with EtOAc. The precipitate was then purified by preparative HPLC (with a linear gradient of 10–60% CH<sub>3</sub>CN in 0.1% aq TFA over 40 min) to give a white powder of compound **20** (16 mg, 25%). <sup>1</sup>H NMR (600 MHz, DMSO-*d*<sub>6</sub>) δ 1.18–1.38 (m, 10H), 1.42–1.54 (m, 7H), 1.58–1.65 (m, 3H), 2.00–2.04 (m, 6H), 2.57 (d, 1H, *J* = 12 Hz), 2.82 (dd, 1H, *J* = 5.0, 12 Hz), 2.99 (q, 4H, *J* = 6.0 Hz), 3.07–3.11 (m, 3H), 3.32–3.37 (m, 2H, overlapping with H<sub>2</sub>O), 4.11–4.13 (m, 1H), 4.30 (dd, 1H, *J* = 5.0, 7.7 Hz), 6.36 (s, 1H), 6.42 (s, 1H), 7.71 (t, 1H, *J* = 5.0 Hz), 7.74 (t, 1H, *J* = 5.0 Hz), 7.83 (t, 1H, *J* = 5.0 Hz); HRMS (ESI): *m/z* 553.3287 (M+H<sup>+</sup>) (calcd for C<sub>25</sub>H<sub>45</sub>N<sub>8</sub>O<sub>4</sub>S: 553.3284).

#### 4.2.12. KPU-252-B1 (**4**)

To a solution of compounds **20** (2.6 mg, 0.0047 mmol) and compound **17** (2.2 mg, 0.0047 mmol) in H<sub>2</sub>O/*t*-butanol/DMF (1:1:1, 0.3 mL) was added Cu(OAc)<sub>2</sub> (5 mol %, 0.042 mg) and sodium ascorbate (15 mol %, 0.14 mg). The reaction mixture was stirred for 15 min at 80 °C under microwave irradiation. After cooling to room temperature, the reaction mixture was diluted with DMSO

and purified by preparative HPLC (with a linear gradient of 35–80% CH<sub>3</sub>CN in 0.1% aq TFA over 40 min) to give a pale yellow powder of the desired probe **4** (3.0 mg, 63%). <sup>1</sup>H NMR (600 MHz, DMSO-*d*<sub>6</sub>) δ 1.15–1.37 (m, 10H), 1.42 (s, 6H), 1.42–1.52 (m, 7H), 1.57–1.63 (m, 1H), 1.79–1.84 (m, 2H), 1.99–2.04 (m, 6H), 2.57 (d, 1H, *J* = 12 Hz), 2.81 (dd, 1H, *J* = 5.2, 12 Hz), 2.92 (q, 2H, *J* = 6.0 Hz), 2.96–3.00 (m, 6H), 3.06–3.10 (m, 1H), 4.12 (dd, 1H, *J* = 4.4, 7.7 Hz), 4.23 (t, 2H, *J* = 6.9 Hz), 4.30 (dd, 1H, *J* = 5.0, 7.5 Hz), 6.36 (br s, 1H), 6.42 (br s, 1H), 6.48 (s, 1H), 6.85 (s, 1H), 7.57–7.60 (m, 3H), 7.65 (s, 1H), 7.66 (s, 1H), 7.69–7.76 (m, 4H), 7.79–7.83 (m, 4H), 8.60 (s, 1H), 10.55 (s, 1H), 11.10 (s, 1H); HRMS (ESI): *m/z* 1018.4969 (M+H<sup>+</sup>) (calcd for C<sub>53</sub>H<sub>68</sub>N<sub>11</sub>O<sub>8</sub>S: 1018.4973).

### 4.3. Tubulin binding assay

Fluorescence spectra were measured at 37 °C as described previously.<sup>11</sup> Porcine tubulin (0.5 μM) in MES buffer (0.1 M MES, 0.5 mM MgCl<sub>2</sub>, 1 mM EGTA, 1 mM GTP, pH 6.8) was incubated with different concentrations of the test compounds (0–12 μM, 1% DMSO) at 37 °C for 1 h. After incubation, the fluorescence of each solution was measured (excitation at 295 nm, emission at 300–450 nm) using an FP-750 Spectrofluorometer (JASCO, JAPAN).

### 4.4. In vitro cytotoxicity assay

The human cell line HT-29 (colorectal adenocarcinoma) was obtained from ATCC. HT-29 cells were maintained in McCoy's 5A medium (modified, Invitrogen) containing 10% fetal bovine serum supplemented with 1% penicillin/streptomycin at 37 °C in a humidified 5% CO<sub>2</sub> atmosphere. For the growth inhibition assays, cells were plated in 96-well plates at 5000 cells/well the day before compound addition. Stock solutions of compounds were prepared in DMSO. Serially diluted compounds were added to the cells, resulting in a final concentration range of 20 μM–2 pM. Seventy-two hours later, 0.1 mg/mL XTT (Sigma) solution in PBS buffer containing 25 μM phenazine methosulfate (Wako) was added to each well and the cells were incubated for an additional 1 h. The absorbance of the formazan product was measured at 492 nm on a plate reader (TECAN SAFIRE). To compensate for the non-specific absorbance, the absorbance at 690 nm was measured.

### 4.5. Tubulin photoaffinity labeling

Tubulin photoaffinity labeling by probe **4** and compound **5** were performed using the same procedure as previously described.<sup>11,12</sup> Briefly, a solution of each compound was added to a tubulin solution (2 μM) in MES buffer (pH 6.8) containing 1 mM GTP and 2% DMSO, and the solution was incubated at 37 °C for 30 min, followed by UV irradiation at 365 nm at a distance of 10 cm on ice for an appropriate time using a UV irradiator.

### 4.6. SDS-PAGE, Western blotting

SDS-PAGE and Western blotting of photolabeled tubulin were performed using the same procedure as described previously.<sup>11,12</sup> Photolabeled tubulin was separated by SDS-PAGE in 10% polyacrylamide gels and transferred to PVDF membrane. The membrane was blocked with 5% (w/v) skim milk in PBS buffer containing 0.1% (v/v) Tween 20 (pH 7.4) and incubated with streptavidin-horseradish peroxidase conjugate (GE healthcare) for 1 h at room temperature to detect the photolabeled protein. After washing, the membrane was incubated with ECL Western blotting detection reagents (GE healthcare), and the chemiluminescence was visualized by using an imaging system (LAS-1000plus, FUJIFILM).

#### 4.7. Competitive photoaffinity labeling with plinabulin, colchicine, vinblastine, and D-biotin

Competitive photoaffinity labeling was performed using the same procedure as described previously.<sup>11</sup> Tubulin (2 μM) was preincubated in the presence or absence of different concentrations of plinabulin, colchicine, vinblastine, or D-biotin in MES buffer for 15 min at 37 °C, followed by addition of probe **4** (2 μM, final concentration 2% DMSO). After incubation at 37 °C for 30 min, samples were UV irradiated at 365 nm at a distance of 10 cm on ice for 30 s, followed by separation by SDS–PAGE. Photolabeled tubulin was visualized in a manner similar to that described above.

#### Acknowledgments

This research was supported by grants from MEXT (Ministry of Education, Culture, Sports, Science and Technology), Japan, including the Grant-in Aid for Young Scientists (B) 21790118 and the Grant-in Aid for Scientific Research (B) 20390036. We are grateful to Professor H. Toyoda, Mr. H. Kikuchi, and Mr. Y. Yoshino at the Tokyo University of Pharmacy and Life Sciences, and Dr. S. Neuteboom at Nereus Pharmaceuticals Inc., who provided HT-29 cells and gave helpful suggestions for the cytotoxicity assay. We also thank Professor Y. Sida and Ms. C. Sakuma of the Tokyo University of Pharmacy and Life Sciences for mass spectra and NMR measurements.

#### Supplementary data

Supplementary data associated with this article can be found, in the online version, at doi:10.1016/j.bmc.2010.10.055.

#### References and notes

- Perez, E. A. *Mol. Cancer Ther.* **2009**, *8*, 2086.
- Jordan, M. A.; Wilson, L. *Nat. Rev. Cancer* **2004**, *4*, 253.
- Zhou, J.; Giannakakou, P. *Curr. Med. Chem. Anticancer Agents* **2005**, *5*, 65.
- Gaya, A. M.; Rustin, G. J. S. *Clin. Oncol.* **2005**, *17*, 277.
- Kanoh, K.; Kohno, S.; Asari, T.; Harada, T.; Katada, J.; Muramatsu, M.; Kawashima, H.; Sekiya, H.; Uno, I. *Bioorg. Med. Chem. Lett.* **1997**, *7*, 2847.
- Kanoh, K.; Kohno, S.; Katada, J.; Takahashi, J.; Uno, I. *J. Antibiot.* **1999**, *52*, 134.
- Kanoh, K.; Kohno, S.; Katada, J.; Hayashi, Y.; Muramatsu, M.; Uno, I. *Biosci., Biotechnol., Biochem.* **1999**, *63*, 1130.
- Kanoh, K.; Kohno, S.; Katada, J.; Takahashi, J.; Uno, I.; Hayashi, Y. *Bioorg. Med. Chem.* **1999**, *7*, 1451.
- Hayashi, Y.; Orikasa, S.; Tanaka, K.; Kanoh, K.; Kiso, Y. *J. Org. Chem.* **2000**, *65*, 8402.
- Nicholson, B.; Lloyd, G. K.; Miller, B. R.; Palladino, M. A.; Kiso, Y.; Hayashi, Y.; Neulteboom, S. T. C. *Anticancer Drugs* **2006**, *17*, 25.
- Yamazaki, Y.; Kohno, K.; Yasui, H.; Kiso, Y.; Akamatsu, M.; Nicholson, B.; Deyanat-Yazdi, G.; Neuteboom, S.; Potts, B.; Lloyd, G. K.; Hayashi, Y. *ChemBioChem* **2008**, *9*, 3074.
- Yamazaki, Y.; Sumikura, M.; Hidaka, K.; Yasui, H.; Kiso, Y.; Yakushiji, F.; Hayashi, Y. *Bioorg. Med. Chem.* **2010**, *18*, 3169.
- (a) Dormán, G.; Prestwich, G. D. *Trends Biotechnol.* **2000**, *18*, 64; (b) Dormán, G.; Prestwich, G. D. *Biochemistry* **1994**, *33*, 5661.
- Huisgen, R. In *1,3-Dipolar Cycloaddition Chemistry*; Padwa, A., Ed.; Wiley: New York, 1984; pp 1–176.
- Rostovtsev, V. V.; Green, L. G.; Fokin, V. V.; Sharpless, K. B. *Angew. Chem., Int. Ed.* **2002**, *41*, 2596.
- Komeyama, K.; Takahashi, K.; Takaki, K. *Org. Lett.* **2008**, *10*, 5119.
- (a) Suzuki, M.; Iwasaki, T.; Miyoshi, M.; Okumura, K.; Matsumoto, K. *J. Org. Chem.* **1973**, *38*, 3571; Makino, K.; Okamoto, N.; Hara, O.; Hamada, Y. *Tetrahedron: Asymmetry* **2001**, *12*, 1757.
- Dess, D. B.; Martin, J. C. J. *Org. Chem.* **1983**, *48*, 4155.
- Loughlin, W. A.; Marshall, R. L.; Carreiro, A.; Elson, K. E. *Bioorg. Med. Chem. Lett.* **2000**, *10*, 91.
- Carboni, B.; Benalil, A.; Vaultier, M. *J. Org. Chem.* **1993**, *58*, 3736.
- (a) Miller, N.; Williams, G. M.; Brimble, M. A. *Org. Lett.* **2009**, *11*, 2409; (b) Miller, N.; Williams, G. M.; Brimble, M. A. *Org. Lett.* **2010**, *12*, 1375.
- (a) Sackett, D. L. *Biochemistry* **1995**, *34*, 7010; (b) Panda, D.; Miller, H. P.; Islam, K.; Wilson, L. *Proc. Natl. Acad. Sci. U.S.A.* **1997**, *94*, 10560.
- Scudiero, D. A.; Shoemaker, R. H.; Paull, K. D.; Monks, A.; Tierney, S.; Nofziger, T. H.; Currens, M. J.; Seniff, D.; Boyd, M. R. *Cancer Res.* **1988**, *48*, 4827.
- Rai, S. S.; Wolff, J. J. *Biol. Chem.* **1996**, *271*, 14707.
- (a) Himes, R. H. *Pharmacol. Ther.* **1991**, *51*, 257; (b) Na, G. C.; Timasheff, S. N. *J. Biol. Chem.* **1982**, *257*, 10387.